

# Dynamic multi-hop multipath RMSA and traffic grooming in OFDM-based sliceable elastic optical networks

Hwa-Chun Lin<sup>a,\*</sup> and Wei-Te Tseng<sup>b</sup>

<sup>a</sup> *Department of Computer Science, National Tsing Hua University, No. 101, Section 2, Kuang-Fu Road, Hsinchu, Taiwan*

*E-mail: [hclin@cs.nthu.edu.tw](mailto:hclin@cs.nthu.edu.tw)*

<sup>b</sup> *Institute of Communications Engineering, National Tsing Hua University, No. 101, Section 2, Kuang-Fu Road, Hsinchu, Taiwan*

Received 22 June 2022

Accepted 11 January 2023

**Abstract.** In elastic optical networks (EON), routing, modulation selection, and spectrum assignment (RMSA) is crucial in provisioning connection requests. Multipath RMSA offers a number of benefits including provisioning of ultra-high bandwidth demands and better utilization of fragmented spectrum resource. By Combining with traffic grooming, multipath RMSA and traffic grooming is able to provide better utilization of network resource in provisioning connection requests. Adding multi-hop routing mechanism to multipath RMSA and traffic grooming increases the flexibility for selecting paths resulting in higher probability of successfully finding routing paths for connection requests. Dynamic multipath RMSA problem in EON has been investigated extensively in the literature. Dynamic multi-hop multipath RMSA and traffic grooming problem in EON is far from been well studied. This paper proposes an algorithm for the dynamic multi-hop multipath RMSA and traffic grooming problem in OFDM-based elastic optical networks with sliceable bandwidth-variable transponders. Performance of the proposed algorithm is studied via simulation. Our simulation results show that the proposed algorithm yields lower bandwidth blocking ratio than an existing algorithm.

Keywords: Dynamic multi-hop multipath RMSA, traffic grooming, elastic optical networks

## 1. Introduction

Elastic optical network (EON) [15] has been proposed to flexibly allocate spectrum of appropriate size to each connection request in order to make efficient utilization of the optical spectrum. Sliceable bandwidth-variable transponder (SBVT) has been proposed to allow multiple optical connections to share the capacity of a single transponder [12,16]. Multiple optical channels with the same source and destination can be packed into a super-channel without guard bands by using an advanced multicarrier transmission technique such as Nyquist-WDM or orthogonal frequency-division multiplexing (OFDM) [16]. This mechanism is referred to as optical grooming.

An OFDM-based optical grooming mechanism that allows multiple optical channels with the same source but different destinations to share a transponder at the source node has been proposed in [35]. No guard band is required along the common portion of the routes of two channels that are allocated on adjacent spectrum slots. When an

---

\*Corresponding author. E-mail: [hclin@cs.nthu.edu.tw](mailto:hclin@cs.nthu.edu.tw).

optical channel travels along a different route from the rest of the channels at an intermediate node, the original optical superchannel is split and guard bands are added beside the separated optical channels.

The problem of finding a routing, modulation selection, and spectrum assignment (RMSA) strategy for an EON to improve a certain performance measure is referred to as the RMSA problem. For networks that support a single modulation format, this problem is known as the RSA problem. Surveys of RSA/RMSA algorithms for EONs can be found in [1,8,28]. Reviews of RSA/RMSA algorithms with traffic grooming for EONs can be found in [1,8,20,28].

The concept of multipath RMSA is to allow the traffic of a connection request to be split into two or more sub-flows, each of which is routed over a separate lightpath. Multipath RMSA offers a number of benefits including provisioning connection requests with ultra-high bandwidth demands [39], single-hop provisioning of long distance and high-bandwidth connection requests [10], and better utilization of fragmented spectral resource [10,11,17]. Note that differential delay between different routing paths can be addressed using differential delay compensation techniques [3] or a multipath provisioning approach that takes differential delay into account. How to address the differential delay issue for multipath provisioning is out of the scope of this paper.

Previous works on multipath RSA in EON that do not consider differential delay bound can be found in [5,9–11,13,14,17,23–25,29,30,33,34,36–39]. Multipath RSA problems studied in these previous works can be classified into static multipath RSA problems [23,24,30,36] or dynamic multipath RSA problems [5,9–11,13,14,17,25,29,33,34,37–39] depending on whether connection requests are given in advance or arrival/terminating dynamically. Most of these previous works considered networks with multiple modulation formats [9,10,13,14,17,23,25,29,30,36–39], i.e., these authors studied multipath RMSA problems. The rest of these previous works considered networks with a single modulation format [5,11,24,33,34]. Among these previous works, traffic grooming mechanisms are employed in [11] and [13]. No traffic grooming mechanism was used in [5,10,14,17,23–25,29,30,33,34,36–39].

The process of finding a source-destination path consisting of a single lightpath is referred to as single-hop routing, where one hop corresponds to a lightpath which may consist of one or more physical hops in the network. For example, Fig. 1(b) shows a path 1–2–3–5 from node 1 to node 5 consisting of a single lightpath  $p_1$ . Each source-destination path found by a single-hop multipath RMSA and traffic grooming algorithm consists of a single lightpath with no O/E/O conversion at any intermediate node as the example shown in Fig. 1(b). On the other hand, the process of finding a source-destination path that may contain multiple lightpaths concatenated together is called multi-hop routing. For example, suppose that there is no sufficient number of continuous spectrum slots along any of the paths 1–4–5, 1–2–3–5, and 1–2–3–4–5 to fulfill the required bandwidth. Suppose that there are sufficient number of continuous spectrum slots along paths 1–2–3 and 3–4–5. Figure 1(c) shows a path 1–2–3–4–5 from node 1 to node 5 consisting of two lightpaths  $p_2$  and  $p_3$  with sufficient number of continuous spectrum slots concatenated together at node 3. Concatenating two or more lightpaths at intermediate nodes requires O/E/O conversions. A multi-hop multipath RMSA and traffic grooming algorithm has the advantage of reducing request blocking ratio at the cost of increasing end-to-end delay and energy consumption for O/E/O conversions. The work in [13] is the only research among these previous works on multipath RMSA and traffic grooming that employs multi-hop routing to provision connection requests. The rest of these previous works employ single-hop routing.

This paper develops an auxiliary graph for the purpose of routing and path selection and proposes a dynamic multi-hop multipath RMSA and traffic grooming algorithm. In contrast to the auxiliary graph proposed in [13], the weights on the edges in the auxiliary graph developed in this paper are based on a novel weight that incorporate spectrum fragmentation status, spectrum misalignment status, and spectrum usage. The contributions of this paper

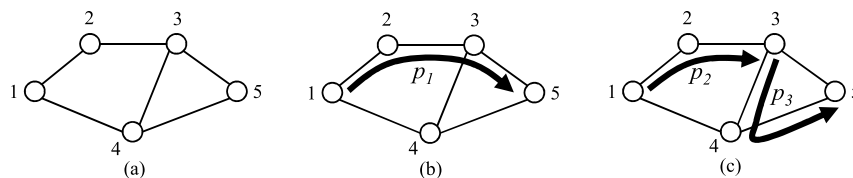


Fig. 1. (a) A network with 5 nodes. (b) Single-hop routing. (c) Multi-hop routing.

are as follows. First of all, this paper proposes a novel lightpath weight that is a combination of the number of spectrum slots, spectrum fragmentation, and spectrum misalignment to assess the potential effect of a lightpath on the availability of network resource. Second, this paper develops an auxiliary graph based on the lightpath weight and proposes a multi-hop multipath RMSA and traffic grooming algorithm based on the auxiliary graph. Finally, via simulation, this paper shows that the proposed dynamic multi-hop multipath RMSA and traffic grooming yields lower bandwidth blocking ratio than best multipath algorithm proposed in [13].

The rest of this paper is organized as follows. The weight assigned to a lightpath will be explained in the next section. The proposed dynamic multi-hop multipath RMSA and traffic grooming algorithm will then be described in Section 3. The worst case computational complexity of the proposed algorithm will be presented in Section 4. The performance of the proposed dynamic multi-hop multipath RMSA and traffic grooming algorithm will be studied in Section 5. Finally, some concluding remarks will be given in Section 6.

## 2. Lightpath weight

A lightpath weight assigned to a lightpath is used to evaluate the potential effect of the spectrum slots occupied by the lightpath on provisioning upcoming connection requests. The lightpath weight is related to (i) the number of spectrum slots occupied by the lightpath, (ii) spectrum fragmentation, and (iii) spectrum misalignment induced by the lightpath. The lightpath weight will be used for assigning weights on the edges in an auxiliary graph in the proposed dynamic multi-hop multipath RMSA and traffic grooming algorithm.

### 2.1. Number of spectrum slots

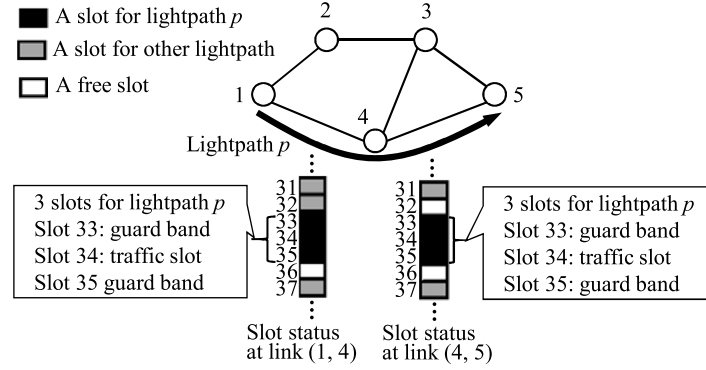
The number of spectrum slots for establishing a lightpath for provisioning a connection request includes the number of spectrum slots for data transmission, the number of reserved spectrum slots (if any), and the number of guard band slots (if any), where the reserved slots are reserved using the spectrum reservation scheme employed in [13]. The number of data slots is calculated based on the bandwidth requirement of the connection request, the selected modulation format, and the symbol rate per subcarrier. The number of guard band slots for the lightpath depends on whether the optical grooming mechanism is used. If the optical grooming mechanism is not used, guard band slots are required around the data slot(s). On the other hand, when the optical grooming mechanism is employed, no guard band is needed to separate the lightpath from the side-by-side lightpath along the common portion of the routes of the two lightpaths [16,35]. Let  $f(p)$  denotes the sum of the number of spectrum slots for carrying the traffic of a lightpath  $p$  and the number of spectrum slots (if any) reserved on lightpath  $p$ . Let the number of guard band slots at link  $l$  on lightpath  $p$  be  $g_l(p)$ . Let the total number of spectrum slots required to establish lightpath  $p$  be denoted by  $\psi(p)$  which is calculated as follows:

$$\psi(p) = h(p)f(p) + \sum_{l \in p} g_l(p), \quad (1)$$

where  $h(p)$  is the number of physical hops of lightpath  $p$ .

For example, lightpath  $p$  in Fig. 2 originated at node 1 and terminated at node 5 along route 1–4–5 consists of two physical hops, i.e.,  $h(p) = 2$ . The status of spectrum slots 31 through 37 are shown in Fig. 2. The status of the rest of spectrum slots are not shown. Suppose that slot 34 at links (1, 4) and (4, 5) is allocated to lightpath  $p$  for carrying traffic and that slots 33 and 35 at the two links are allocated as guard bands, i.e.,  $f(p) = 1$ ,  $g_{(1,4)}(p) = 2$ , and  $g_{(4,5)}(p) = 2$ . Thus, the total number of spectrum slots required to establish lightpath  $p$  in Fig. 2 is calculated as  $\psi(p) = 2 \times 1 + 2 + 2$ , i.e.,  $\psi(p) = 6$ .

The total number of spectrum slots required to establish a lightpath  $p$  is normalized to a value between 0 and 1 by dividing it by its largest possible value. The widest lightpath can occupy all spectrum slots supported by a sliceable transponder. Let  $S_t$  denote the number of spectrum slots supported by a sliceable transponder. This paper

Fig. 2. A lightpath  $p$  in a network with 5 nodes.

uses one of the  $K$  shortest routes between the originating and terminating nodes to establish a lightpath. Let  $H$  be the hop count of the route with the largest number of physical hops among the  $K$  shortest routes between any pair of nodes. The largest possible number of spectrum slots for establishing a lightpath is  $S_t H$ . The normalized number of spectrum slots required to establish a lightpath  $p$ ,  $\tilde{\psi}(p)$ , is calculated as follows:

$$\tilde{\psi}(p) = \frac{\psi(p)}{S_t H}. \quad (2)$$

Suppose that two shortest paths between any pair of nodes in the example network in Fig. 2 are used for establishing lightpaths, i.e., the value of  $K$  is 2. For the example network shown in Fig. 2, the route with the largest number of physical hops among the  $K$  ( $K = 2$ ) shortest routes between any pair of nodes is 3, i.e.,  $H = 3$ . Suppose that the number of spectrum slots supported by a sliceable transponder is 10, i.e.,  $S_t = 10$  which is also the largest possible number of spectrum slots for establishing a lightpath. Thus, the normalized number of spectrum slots required to establish lightpath  $p$  in Fig. 2 is calculated as  $\tilde{\psi}(p) = 6/(10 \times 3) = 0.2$ , i.e.,  $\tilde{\psi}(p) = 0.2$ .

## 2.2. Spectrum fragmentation

Spectrum fragments of various sizes in terms of spectrum slots are created as lightpaths are established and torn down dynamically. Compared with a spectrum fragment of small size, a spectrum fragment of large size is more flexible for provisioning upcoming connection requests with different bandwidth requirements. A spectrum fragment of large size also has larger number of alternatives for accommodating a connection request with a given bandwidth requirement. It is preferable to use a smaller spectrum fragment to establish a lightpath to provision a connection request leaving spectrum fragments of larger sizes for upcoming connection requests.

This paper defines the fragmentation cost of a lightpath as the sum of the sizes of the spectrum fragments created by the lightpath. Let  $\phi_l(p)$  be the fragmentation cost of lightpath  $p$  at link  $l$ , which is the sum of the numbers of contiguous free spectrum slots (if any) with immediate lower and higher spectrum indices than the spectrum slots used by lightpath  $p$  at link  $l$ . Let the number of contiguous free spectrum slots (if any) with immediate lower indices than the spectrum slots used by lightpath  $p$  at link  $l$  be denoted by  $x_l(p)$  and the number of contiguous free spectrum slots with immediate higher indices than the spectrum slots used by lightpath  $p$  at link  $l$  be denoted by  $y_l(p)$ . If the lowest indexed spectrum slot is allocated to lightpath  $p$  at link  $l$ ,  $x_l(p)$  is zero. Similarly, if the highest indexed spectrum slot is allocated to lightpath  $p$  at link  $l$ ,  $y_l(p)$  is zero. Let  $\phi(p)$  be the fragmentation cost of lightpath  $p$ , which is calculated as follows:

$$\phi(p) = \sum_{l \in p} \phi_l(p) = \sum_{l \in p} (x_l(p) + y_l(p)). \quad (3)$$

The fragmentation cost of lightpath  $p$  is normalized to a value between 0 and 1 by dividing it by its largest possible value. The largest possible value of the fragmentation cost of a lightpath  $p$  is less than the number of spectrum slots on an optical fiber multiplied by  $H$ . Let the number of spectrum slots on an optical fiber be denoted by  $S_f$ . The normalized fragmentation cost of lightpath  $p$ ,  $\tilde{\phi}(p)$ , is calculated as follows:

$$\tilde{\phi}(p) = \frac{\phi(p)}{S_f H}. \quad (4)$$

For the example network and lightpath  $p$  in Fig. 2, the number of contiguous free spectrum slots with immediate lower indices than the spectrum slots used by lightpath  $p$  at link (1, 4) is 0, i.e.,  $x_{(1,4)}(p) = 0$ . the numbers of contiguous free spectrum slots with immediate higher indices than the spectrum slots used by lightpath  $p$  at link (1, 4) is 1, i.e.,  $y_{(1,4)}(p) = 1$ . Similarly, the numbers of contiguous free spectrum slots with immediate lower and higher indices than the spectrum slots used by lightpath  $p$  at link (4, 5) are respectively 1 and 1, i.e.,  $x_{(4,5)}(p) = 1$  and  $y_{(4,5)}(p) = 1$ . Thus, the fragmentation cost of lightpath  $p$  in Fig. 2 is calculated as  $\phi(p) = 0+1+1+1 = 3$ , i.e.,  $\phi(p) = 3$ . Suppose that the number of spectrum slots on an optical fiber is 320, i.e.,  $S_f = 320$ . Recall that the route with the largest number of physical hops among the  $K$  ( $K = 2$ ) shortest routes between any pair of nodes in the example network is 3, i.e.,  $H = 3$ . The normalized fragmentation cost of lightpath  $p$  in Fig. 2 is calculated as  $\tilde{\phi}(p) = 3/(320 \times 3)$ , i.e.,  $\tilde{\phi}(p) = 1/320$ .

### 2.3. Spectrum misalignment

The concept of spectrum ‘‘misalignment’’ has been described in [31,32] as one that breaks the continuity of available spectrum slots between a link and a neighbor link when a lightpath is established. The definition of the number of spectrum misalignments in [32] counts the number of breaks of spectrum continuity created due to the establishment of the lightpath. While the definition in [31] adds the number of spectrum misalignments created and deducts the number of spectrum misalignments vanished due to the establishment of the lightpath. We are concerned with the effect of the spectrum misalignments created by a lightpath on the provision of upcoming connection requests. Thus, this paper adopts the definition in [32].

Let  $\alpha_l(p)$  denote the number of misalignments created at link  $l$  on lightpath  $p$ . The total number of misalignments created by lightpath  $p$ ,  $\alpha(p)$ , is calculated as

$$\alpha(p) = \sum_{l \in p} \alpha_l(p). \quad (5)$$

For example, Fig. 3(b) shows that, when spectrum slots 33, 34, and 35 are allocated to lightpath  $p$  at link (1, 4), the spectrum continuity of free slots 33 and 34 between links (2, 1) and (1, 4) are broken and that the spectrum continuity of free slots 34 and 35 between links (1, 4) and (4, 3) are broken. Figure 3(c) shows that, when spectrum slots 33, 34, and 35 are allocated to lightpath  $p$  at link (4, 5), the spectrum continuity of free slot 35 between links (3, 4) and (4, 5) is broken and that the spectrum continuity of free slots 34 and 35 between links (4, 5) and (5, 3) are broken. Thus, the allocation of spectrum slots 33, 34, and 35 to lightpath  $p$  creates a total of 7 misalignments, i.e.,  $\alpha(p) = 7$ .

The total number of misalignments created by lightpath  $p$  is normalized to a value between 0 and 1 by dividing it by the maximum number of misalignments that can be created by a lightpath. To find the maximum possible number of misalignments, we assume that the degree of all of the nodes in the network are  $D$ , where  $D$  is the largest degree of the nodes in the network. The maximum number of spectrum slots that can be used to establish a light path is the maximum number of spectrum slots supported by a transponder  $S_t$ . The maximum number of misalignments that can be created at the first or the last link on a lightpath is  $S_t(D - 1 + D - 2)$ , i.e.,  $S_t(2D - 3)$ . The maximum number of misalignments that can be created at one of the rest of the links on the lightpath is  $2S_t(D - 2)$ . Thus, the maximum number of misalignments that can be created by a lightpath  $p$  with  $H$  physical hops is

$$S_t[4D - 6 + 2(H - 2)(D - 2)]. \quad (6)$$

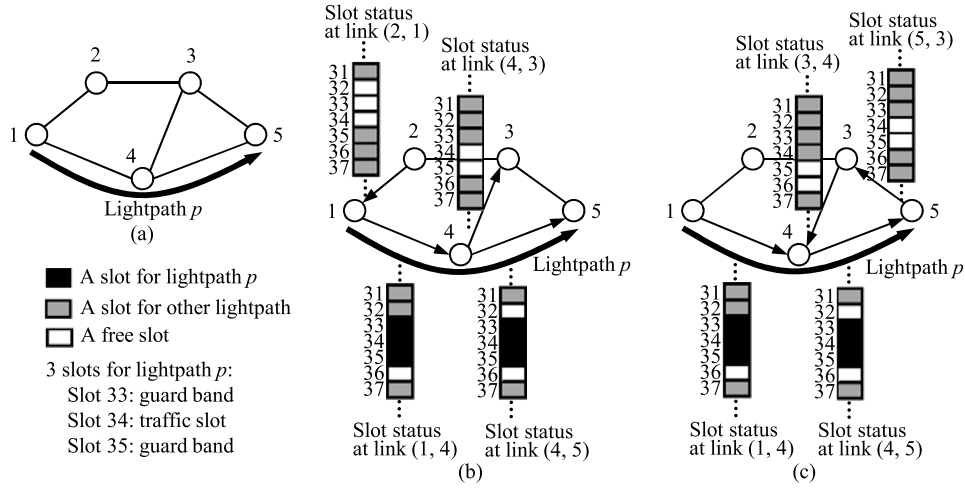


Fig. 3. (a) A lightpath  $p$  in a network with 5 nodes. (b) Misalignments created due to the allocation of slots 33, 34, and 35 to lightpath  $p$  at link (1, 4). (c) Misalignments created due to the allocation of slots 33, 34, and 35 to lightpath  $p$  at link (4, 5).

Let  $\tilde{\alpha}(p)$  denote the normalized number of misalignments created by lightpath  $p$ , which is calculated as

$$\tilde{\alpha}(p) = \frac{\alpha(p)}{S_t[4D - 6 + 2(H - 2)(D - 2)]}. \quad (7)$$

The largest degree of the nodes in the network in Fig. 3 is 3, i.e.,  $D = 3$ . Again, suppose that the number of spectrum slots supported by a sliceable transponder is 10, i.e.,  $S_t = 10$  which is also the largest possible number of spectrum slots for establishing a lightpath. Recall that the route with the largest number of physical hops among the  $K$  ( $K = 2$ ) shortest routes between any pair of nodes in the example network is 3, i.e.,  $H = 3$ . The normalized number of misalignments created by lightpath  $p$  is calculated as  $\tilde{\alpha}(p) = 7/(10(4 \times 3 - 6 + 2(3 - 2)(3 - 2))) = 7/80$ , i.e.,  $\tilde{\alpha}(p) = 7/80$ .

The larger the number of spectrum misalignments in the network, it is more difficult for an RSA/RMSA algorithm to find a routing path that satisfies the spectrum continuity constraint. Thus, it is preferable to use a lightpath that yields smaller number of spectrum misalignments to provision a connection request. Hopefully, the RSA/RMSA algorithm has higher probability to successfully find lightpaths(s) to provision upcoming connection requests.

In recent years, the channel slicing and stitching technology [6] has been proposed to remove the spectrum continuity constraint such that misaligned spectrum slots can be allocated to a lightpath. If this technology is adopted in an EON network in which all nodes are equipped with sufficient number of splitting components and stitching components such that splitting process and stitching process can be performed whenever required even at intermediate nodes along any routing path, the spectrum continuity constraint can be completely removed and the spectrum-misalignment term in the lightpath weight can be dropped. However, if the splitting process or stitching process cannot be carried out at any of the nodes when required (i.e., the spectrum continuity constraint must be observed at the node for certain pair of links), the spectrum-misalignment term can be used to reflect this effect to some extent. Example situation where splitting process may not be able to be performed is that each node in the network is equipped with a limited number of slicers [2, 18] or that only a subset of the nodes in the network are equipped with slicers [2]. In the EON networks considered in this paper, the channel slicing and stitching technology is not adopted.

#### 2.4. Lightpath weight of a lightpath $p$

Calculation of the lightpath weight of a lightpath  $p$  depends on whether  $p$  is an existing lightpath or a candidate lightpath to be established. Let  $z(p)$  be the lightpath weight of a lightpath  $p$ . For a candidate lightpath  $p$ , its lightpath weight is calculated as the sum of the normalized fragmentation cost, normalized number of misalignments, and normalized number of spectrum slots of lightpath  $p$ , i.e.,

$$z(p) = \tilde{\phi}(p) + \tilde{\alpha}(p) + \tilde{\psi}(p). \quad (8)$$

For an existing lightpath  $p$ , grooming traffic onto  $p$  electrically does not create additional spectrum fragmentation or misalignment or occupy extra spectrum slots. Among different existing lightpaths that can be used to provision the traffic, it is desirable to use an existing light path that occupies smaller number of spectrum slots. Therefore, the normalized number of spectrum slots of existing lightpath  $p$  is used as its lightpath weight, i.e.,

$$z(p) = \tilde{\psi}(p). \quad (9)$$

### 3. Dynamic multi-hop multipath RMSA and traffic grooming algorithm

In the proposed algorithm, each path used to provision a connection request may consist of a single lightpath or multiple concatenated lightpaths. The proposed algorithm first tries to use a single path with sufficient bandwidth to provision a connection request. If the connection request cannot be fulfilled using a single path, the proposed algorithm tries to find multiple paths to provision the connection request. The proposed dynamic multi-hop multipath RMSA and traffic grooming algorithm finds each path based on an auxiliary graph. In the following, the auxiliary graph will first be described. The multi-hop multipath RMSA and traffic grooming algorithm will then be given.

#### 3.1. Auxiliary graph

An auxiliary graph is constructed based on the topology of the network, a target bandwidth to be satisfied, and the resource status of the network. The target bandwidth for constructing an auxiliary graph is either the remaining bandwidth of a connection request to be satisfied or the bandwidth of a maximum bandwidth path from the source node to the destination node of the connection request, whichever is smaller. The target bandwidth for constructing an auxiliary graph is denoted by  $b_t$ . Each node in the network has a corresponding vertex in the auxiliary graph. The edges in the auxiliary graph are classified into single-lightpath edges and multi-lightpath edges.

##### 3.1.1. Single-lightpath edge

It is preferable to use an existing lightpath with sufficient residual bandwidth to provision a connection request. If there is at least one existing lightpath from node  $i$  to node  $j$  with residual bandwidth greater than or equal to the target bandwidth  $b_t$ , select the one with the least lightpath weight with ties broken arbitrarily and add a single-lightpath edge from vertex  $i$  to vertex  $j$ . Otherwise, try to find all candidate lightpaths, including candidate lightpaths using optical grooming and without using optical grooming, with just enough number of spectrum slots to support a bandwidth of  $b_t$  along the  $K$ -shortest physical paths from node  $i$  to node  $j$ . The spectrum reservation scheme used in [13] is employed to reserved spectrum slots. If at least one such candidate lightpath is found, select the one with the largest capacity and add a single-lightpath edge from vertex  $i$  to vertex  $j$ . Ties are broken by choosing the candidate lightpath with the least lightpath weight with further ties broken arbitrarily.

Figure 4(a) show a network with 5 nodes. Suppose that an existing lightpath with residual bandwidth greater than or equal to the target bandwidth  $b_t$  or a candidate lightpath with a capacity greater than or equal to the target bandwidth  $b_t$  can be found between each of the following node pairs: (1, 2), (1, 4), (2, 1), (3, 1), (4, 1), (4, 3), (5, 1), (5, 3), and (5, 4), where  $(s, d)$  is a source-destination pair with source node  $s$  and destination node  $d$ . A directed single-lightpath edge is added between each of these node pairs in the auxiliary graph as shown in Fig. 4(b).

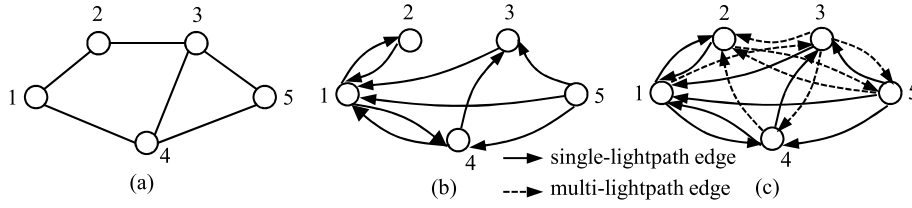


Fig. 4. (a) A network with 5 nodes. (b) Auxiliary graph with only single-lightpath edges. (c) Auxiliary graph with single-lightpath and multi-lightpath edges.

### 3.1.2. Multi-lightpath edge

An attempt is made to add a multi-lightpath edge from vertex  $i$  to vertex  $j$  only when a single-lightpath edge has not been added. The flowchart for trying to add a multi-lightpath edge from vertex  $i$  to vertex  $j$  is presented in Fig. 5.

All exiting lightpaths from node  $i$  to node  $j$  are sorted according to their residual bandwidths with ties broken by giving priority to existing lightpaths with lower lightpath weights. Select one or more existing lightpaths until the aggregated residual bandwidth is greater than or equal to the target bandwidth  $b_t$  or the upper limit on the number of existing lightpaths  $L$  is reached. In this paper, the value of  $L$  is selected to be 5. If the aggregated residual bandwidth of the selected existing lightpath(s) is greater than or equal to  $b_t$ , a multi-lightpath edge from vertex  $i$  to vertex  $j$  is added in the auxiliary graph to represent the set of selected existing lightpath(s).

If the aggregated residual bandwidth of the selected existing lightpath(s) is less than  $b_t$ , one or more candidate lightpaths are needed such that the aggregated residual bandwidth of the selected existing lightpath(s) and candidate lightpath(s) is greater than or equal to  $b_t$ . Note that no single candidate lightpath is able to provide a bandwidth of  $b_t$  since no single-lightpath edge from vertex  $i$  to vertex  $j$  was added. Find all candidate lightpaths, including candidate lightpaths using optical grooming and without using optical grooming, along the  $K$ -shortest physical paths from node  $i$  to node  $j$  and sort them in descending order of their capacities with ties broken by giving priority to candidate lightpaths with lower lightpath weights. The spectrum reservation scheme used in [13] is employed to reserved spectrum slots. Select one or more candidate lightpaths until the sum of the residual bandwidths of the selected existing lightpath(s) and capacities of the selected candidate lightpath(s) is greater than or equal to  $b_t$  or there no candidate left to be selected. If the sum of the residual bandwidths of the selected existing lightpath(s) and capacities of the selected candidate lightpath(s) is less than  $b_t$ , no multi-lightpath edge from vertex  $i$  to vertex  $j$  is added.

If the sum of the residual bandwidths of the selected existing lightpath(s) and capacities of the selected candidate lightpath(s) is greater than or equal to  $b_t$ , it is possible that one or more selected existing lightpaths can be removed such that the aggregated bandwidth of the remaining selected lightpaths is still greater than or equal to  $b_t$  since the lightpaths are selected in two different stages. It is obvious that none of the candidate lightpath(s) can be removed since they are selected in the second stage. If the aggregated capacity of the selected candidate lightpath(s) is greater than or equal to  $b_t$ , all selected existing lightpath(s) can be removed. Otherwise, sort the previously selected existing lightpath(s) in descending order of their residual bandwidths and select one or more existing lightpaths until the sum of the residual bandwidths of the selected existing lightpath(s) and capacities of the selected candidate lightpath(s) is greater than or equal to  $b_t$ . The rest of the previously selected existing lightpaths (if any) that are not selected at this stage are removed. A multi-lightpath edge from vertex  $i$  to vertex  $j$  is added in the auxiliary graph to represent the set of selected lightpath(s).

In Fig. 4(b), no single-lightpath edge was added between each of the following node pairs: (1, 3), (1, 5), (2, 3), (2, 4), (2, 5), (3, 2), (3, 4), (3, 5), (4, 2), (4, 5), and (5, 2). An attempt is made to find a set of lightpaths with aggregated bandwidth greater than or equal to  $b_t$  between each of these node pairs. Suppose that this attempt is successful for each of the following node pairs: (1, 3), (2, 5), (3, 2), (3, 4), (3, 5), (4, 2), and (5, 2). A directed multi-lightpath edge is added between each of these node pairs as shown in Fig. 4(c). Figure 4(c) also shows that no edge appears between each of the following node pairs: (1, 5), (2, 3), (2, 4), and (4, 5).

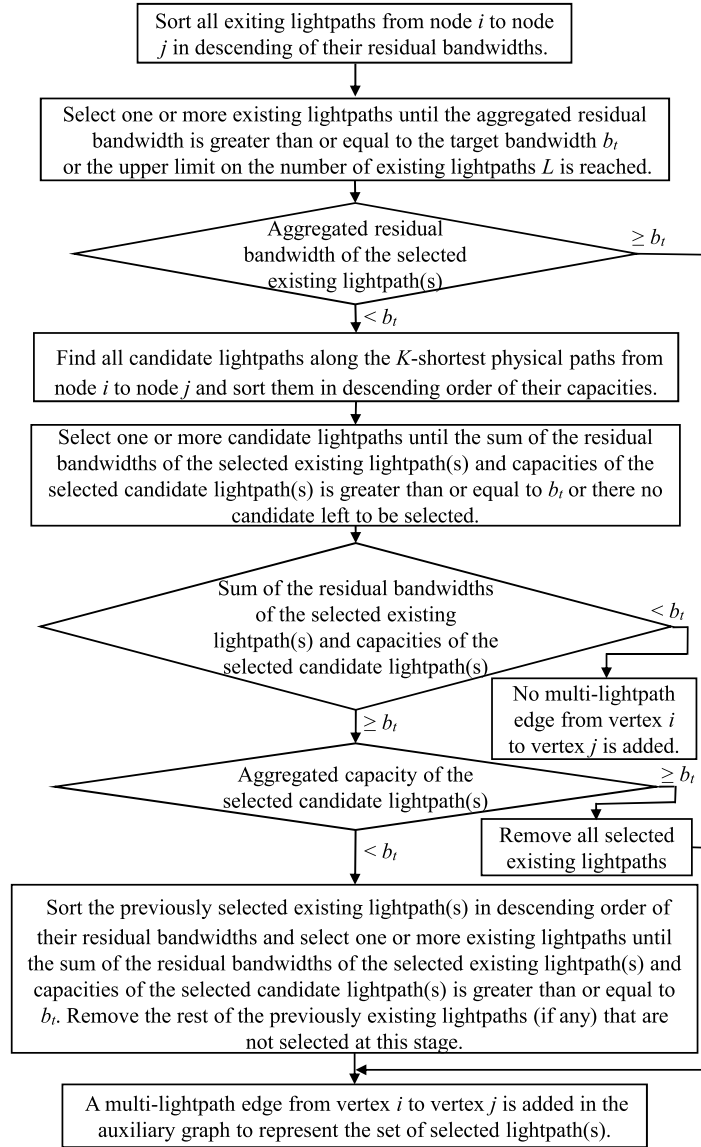


Fig. 5. The flowchart for trying to add a multi-lightpath edge from vertex  $i$  to vertex  $j$  in the auxiliary graph.

### 3.1.3. Edge weights

The weight on an edge in the auxiliary graph is assigned based on the sum of the lightpath weight(s) of the set of lightpath(s) it represents. Using existing lightpath(s) to provision a connection request is preferable than establishing new lightpath(s). Thus, a large constant is added to the weight of an edge for each candidate lightpath in the set of lightpath(s) it represents in addition to the total lightpath weights of the lightpath(s) in the set. The value of the constant is selected such that the sum of the constant and the lightpath weight of a candidate lightpath is larger than sum of the lightpath weights of the largest possible number of existing lightpaths.

### 3.2. The algorithm

When a connection request  $(s, d, b)$  with source node  $s$ , destination node  $d$ , and requested bandwidth  $b$  arrives, the proposed dynamic multi-hop multipath RMSA and traffic grooming algorithm constructs one or more auxiliary graphs and tries to find one or more paths to provision the connection request. Let  $b_r$  be the remaining bandwidth of the connection request to be satisfied, which is initially  $b$ . An upper limit  $N_{sd}$  is placed on the number of source-to-destination paths in the auxiliary graphs used to provision a single connection request to prevent the coexistence of too many lightpaths in the network since a larger number of lightpaths requires more spectrum for guard bands. A source-to-destination path in an auxiliary graph will be referred to as an  $sd$ -path for simplicity. Let  $n_{sd}$  denote the number of  $sd$ -paths found so far in the algorithm.

Two types of auxiliary graphs are used in the algorithm for finding one or more  $sd$ -paths to provision the connection request. The first type of auxiliary graphs consists of only single-lightpath edges among the node pairs. The second type of auxiliary graphs contains both single-lightpath and multi-lightpath edges among the node pairs. Let  $\Omega$  denote the type of auxiliary graphs. The value of  $\Omega$  is either  $S$  representing the first type or  $B$  denoting the second type. Let  $AG(\Omega, b_t)$  denote an auxiliary graph of type  $\Omega$ , in which the set of lightpaths represented by each edge is found based on a target bandwidth of  $b_t$ .

The proposed dynamic multi-hop multipath RMSA and traffic grooming algorithm is given in Algorithm 1. The proposed algorithm consists of a single-path phase and a multi-path phase. The term ‘‘single-path phase’’ is

---

#### Algorithm 1 Multi-hop algorithm

---

1. Set  $n_{sd} = 0$ ,  $b_r = b$ ,  $b_t = b$ ,  $FirstIteration = true$ , and  $STOP = false$ .
  2. **Repeat**
  3.   **If**  $FirstIteration = false$
  4.     (a) Construct a bandwidth-based auxiliary graph  $AG(B, b_t)$ .
  5.     (b) Find a max-bandwidth path from  $s$  to  $d$  in the auxiliary graph.  
      Let  $\hat{b}$  be the bandwidth of the max-bandwidth path.
  6.     (c) **If**  $\hat{b} = 0$ , block the connection request.
  7.       Set  $STOP = true$ .
  8.       **Continue** to test the condition of Repeat loop.
  9.       **Else** set  $b_t = \min(\hat{b}, b_r)$ .
  10.    **EndIf**
  11. **EndIf**
  12. **For**  $\Omega$  in  $\{S, B\}$
  13.    Construct an auxiliary graph  $AG(\Omega, b_t)$ .
  14.    Find a shortest path from vertex  $s$  to vertex  $d$  in the auxiliary graph.
  15.    **If** a shortest path can be found
  16.     (a) Use the lightpaths represented by the edges along the shortest path to provision (or partially provision) the connection request.
  17.     (b) Update  $b_r$ . Increment  $n_{sd}$  by one.
  18.     (c) **If**  $b_r = 0$ , accept the connection request.
  19.       Set  $STOP = true$ .
  20.     (d) **ElseIf**  $n_{sd} = N_{sd}$ , block the connection request. Set  $STOP = true$ .
  21.     **EndIf**
  22.     (e) **Break** out of For loop.
  25.    **EndIf**
  26. **EndFor**
  27. Set  $FirstIteration = false$ .
  28. **Until**  $b_r = 0$  or  $n_{sd} = N_{sd}$  or  $STOP = true$ .
-

referring to the process of finding a single sd-path in the auxiliary graph. Similarly, the term “multi-path phase” is referring to the process of finding multiple sd-paths in the auxiliary graphs. The two phases are combined into a single iterative procedure (the Repeat-Until loop, lines 2 through 28). The first iteration of the algorithm is the single-path phase and the rest iterations belong to the multi-path phase. The multi-path phase is performed only when the single-path phase is unable to find a sd-path to provision the connection request.

Each iteration of the multi-hop algorithm consists of two parts. The first part of each iteration corresponds to the first loop of the For loop (lines 12 through 26) in which  $\Omega = S$ . The second part consists of the second loop of the For loop in which  $\Omega = B$ . In the first part, the algorithm uses an auxiliary graph consisting of only single-lightpath edges to try to find a sd-path. The second part is executed only when the first part is not able to find a sd-path. In the second part, the algorithm uses an auxiliary graph containing both single-lightpath edges and multi-lightpath edges to try to find a sd-path.

The target bandwidth  $b_t$  for constructing an auxiliary graph need to be determined before constructing an auxiliary graph. In the first iteration, the target bandwidth  $b_t$  for constructing an auxiliary graph is set to the requested bandwidth  $b$  (line 1). In the rest iterations, the target bandwidth  $b_t$  is determined at the beginning (lines 4 through 9) of each iteration.

At the beginning of each iteration except the first iteration, the algorithm finds the bandwidth of a maximum bandwidth path from the source node  $s$  to the destination node  $d$  by constructing a slightly different auxiliary graph and solves a max-bandwidth path problem [19] (lines 4 and 5). The auxiliary graph consists of both single-lightpath and multi-lightpath edges among the node pairs based on a target bandwidth of  $b_t$  with a slight different criterion in adding a multi-lightpath edge between a node pair. A multi-lightpath edge is added between a node pair regardless of whether the total bandwidth of the selected existing lightpath(s) and candidate lightpath(s) is greater than or equal to the target bandwidth or not. The weight assigned on each edge is the total bandwidth of the set of lightpaths represented by the edge. This auxiliary graph will be referred to as a *bandwidth-based* auxiliary graph. The algorithm then finds a path with the maximum bandwidth from source node  $s$  to destination node  $d$  using the bandwidth-based auxiliary graph by solving a max-bandwidth path problem [19].

Let  $\hat{b}$  denote the bandwidth of the max-bandwidth path from node  $s$  to node  $d$ . If  $\hat{b}$  is zero (lines 6 through 8), the connection request is blocked since there is not enough available bandwidth to fully provision the connection request. Otherwise (line 9), the target bandwidth  $b_t$  for constructing an auxiliary graph is set to  $\hat{b}$  or the remaining bandwidth to be satisfied  $b_r$ , whichever is smaller.

Then the first part of each iteration (the first loop of the For loop) tries to find a sd-path from source node  $s$  to destination node  $d$  in an auxiliary graph consisting of only single-lightpath edges among the node pairs (lines 13 and 14). If no sd-path can be found, the algorithm continues with the second part of the current iteration (the second loop of the For loop). On the other hand, if a sd-path can be found in the first part (line 15), the algorithm (i) uses the lightpaths represented by the edges along the sd-path to provision (or partially provision) the connection request (line 16), (ii) increments the number of sd-paths by one (line 17), (iii) updates the remaining bandwidth to be satisfied (line 17). If the remaining bandwidth to be satisfied is zero, accept the connection request and terminate the algorithm (lines 18 through 19). If the number of sd-paths reaches the upper limit  $N_{sd}$  and the remaining bandwidth is not completely satisfied, block the connection request and terminate the algorithm (lines 20 and 21). If the requested bandwidth is not completely fulfilled and the number of sd-paths is less than the upper limit  $N_{sd}$ , proceed to the next iteration in the Repeat-Until loop (line 22). The second part of each iteration (the second loop of the For loop) employs an auxiliary graph consisting of both single-lightpath edges and multi-lightpath edges among the node pairs to try to find a sd-path from node  $s$  to node  $d$  (lines 13 and 14). The rest operations of the second part of each iteration are the same as those of the first part of each iteration. The algorithm continues iteratively until the requested bandwidth is completely fulfilled or the connection request is blocked.

Figure 4 can be used as an example to briefly explain the proposed multi-hop multipath RMSA and traffic grooming algorithm. Let node 1 be the source node and node 5 be the destination node of an incoming connection request with a bandwidth requirement of  $b$ . Suppose that the first iteration of the Repeat-Until loop is not able to find any sd-path with sufficient bandwidth to provision the connection request, i.e., both the first and second loop of the For loop are unable to find a sd-path. The algorithm enters the second iteration of the Repeat-Until loop.

The algorithm finds the bandwidth,  $\hat{b}$ , of a maximum bandwidth path from node 1 to node 5, which must be less than  $b$  since the first iteration of the Repeat-Until loop is unable to find a sd-path with sufficient bandwidth. Hence, the target bandwidth  $b_t$  for constructing an auxiliary graph is set to  $\hat{b}$ . The algorithm then proceeds to the For loop. Suppose that the first loop ( $\Omega = S$ ) of the For loop constructs an auxiliary graph as shown in Fig. 4(b). No sd-path from node 1 to node 5 can be found in the auxiliary graph shown in Fig. 4(b). The second loop ( $\Omega = B$ ) of the For loop constructs an auxiliary graph as shown in Fig. 4(c). Suppose that a shortest sd-path 1–2–5 is found in the auxiliary. The set of the lightpaths represented by the single-lightpath edge (1, 2) and multi-lightpath edge (2, 5) is used to partially provision the connection request. The algorithm then proceeds to the next iteration of the Repeat-Until loop until the condition ( $b_r = 0$  or  $n_{sd} = N_{sd}$  or  $STOP = \text{true}$ ) in line 28 of the algorithm is satisfied.

#### 4. Computational complexity

The two most time consuming operations in the dynamic multi-hop multipath algorithm are constructing auxiliary graphs and finding sd-paths in auxiliary graphs. In the worst case, there are two directed edges connecting each pair of vertices in an auxiliary graph, one in each direction. Each edge represents one or more existing lightpaths or candidate lightpaths or both. In the worst case, the algorithm needs to find all candidate lightpaths between a pair of nodes and calculate their lightpath weights.

The weight of each candidate lightpath can be calculated in the process of finding the candidate lightpath. The worst case complexity for calculating the lightpath weight of a candidate lightpath is dominated by that of the computation of the spectrum misalignment term which involves checking the continuity status between the spectrum slots of a lightpath on a link and the same spectrum slots on neighboring links. To find all candidate lightpaths and their lightpath weights along the  $K$  shortest physical paths between  $s$  and  $d$ , the algorithm needs to go through all  $K$  shortest paths, all physical hops of each path, all spectrum slots at each link and its neighboring links. Hence, the worst case complexity for finding all candidate lightpaths along the  $K$  shortest physical paths between a pair of nodes and calculating their lightpath weights is of  $O(KHDS_f)$ .

As described previously, the worst case computational complexity for finding all candidate lightpaths between a pair of nodes and calculating their lightpath weights is of  $O(KHDS_f)$ . Let  $V$  be the number of nodes in the network. There are  $O(V^2)$  source-destination pairs in the network. Hence, the worst case computational complexity for constructing an auxiliary graph is of  $O(V^2KHDS_f)$ . The multi-hop multipath algorithm finds a maximum of  $N_{sd}$  sd-paths each in one auxiliary graph. Thus, the worst case computational complexity for the multi-hop multipath algorithm to construct auxiliary graphs is of  $O(N_{sd}V^2KHDS_f)$ .

The worst case computational complexity for finding a shortest sd-path in an auxiliary graph using the best shortest path algorithm is of  $O(E+V \log V)$  where  $E$  is the maximum number of edges in an auxiliary graph. Hence, the worst case computational complexity for finding a shortest sd-path in an auxiliary graph using the best shortest path algorithm is of  $O(V^2+V \log V)$ . Thus, for the multi-hop multipath algorithm that finds a maximum of  $N_{sd}$  sd-paths, the worst case computational complexity for finding a maximum of  $N_{sd}$  sd-paths is of  $O(N_{sd}V^2+N_{sd}V \log V)$ .

It is obvious that constructing auxiliary graphs has higher computational complexity than finding sd-paths in auxiliary graphs. Thus, the worst case computational complexity of the multi-hop multipath is dominated by that for constructing auxiliary graphs which is of  $O(N_{sd}V^2KHDS_f)$ .

#### 5. Performance study

The performance of the proposed dynamic multi-hop multipath RMSA and traffic grooming algorithm is studied via simulation. The performance of the proposed dynamic multi-hop multipath RMSA and traffic grooming algorithm is compared with that of an algorithm proposed in [13] since this is the only work that employs multi-hop routing among the previous works [5,9–11,13,14,17,33,34,37–39] on dynamic multipath RSA in EON. Among

the three dynamic multi-hop multipath RMSA and traffic grooming algorithms proposed in [13], the MP-MSU algorithm yields the lowest request blocking ratio. Therefore, the performance of the algorithm proposed in this paper is compared with that of the MP-MSU algorithm proposed in [13]. Three versions of the proposed algorithm with three different values, namely, 1, 3, and infinity, for the limit on the number of sd-paths in the auxiliary graphs,  $N_{sd}$ , are studied. In the simulation results to be given in the following, the three versions of the proposed dynamic multi-hop multipath RMSA and traffic grooming algorithm will be respectively labeled as “MHMP-1”, “MHMP-3”, and “MHMP-inf”.

Four performance measures, namely, bandwidth blocking ratio, spectrum utilization factor, sub-transponder utilization factor, and average number of existing lightpaths per request are used in the simulation study. Ninety-five percent confidence interval is calculated for each data point obtained in the simulation results. The bandwidth blocking ratio is calculated as the total requested bandwidth of blocked connection requests to the total requested bandwidth of all connection requests.

The spectrum utilization factor is calculated in the following way. Let  $P$  be the set of lightpaths established during the simulation time and  $p_i \in P$  be the  $i$ th lightpath in  $P$ . Recall that the number of spectrum slots allocated to lightpath  $p_i$  is  $\psi(p_i)$  as defined in equation (1). Let  $t(p_i)$  be the holding time of lightpath  $p_i$ . The holding time of a lightpath can be obtained during the simulation by subtracting the time at which the lightpath is established from the time at which it is torn down when no connection is using the lightpath. Let  $T$  be the length of the simulation time. The spectrum utilization factor is calculated as the following ratio

$$\frac{\sum_{p_i \in P} \psi(p_i)t(p_i)}{LS_f T}, \quad (10)$$

where  $L$  is total number of directed links (or optical fibers) in the network. Recall that  $S_f$  is the number of spectrum slots on each directed link (or optical fiber). The numerator in equation (10) can be accumulated during the simulation whenever a lightpath is torn down.

The sub-transponder utilization factor is computed in the following manner. Let the number of transponders (or SBVTs) in the network be denoted by  $\Theta$  and the number of sub-transponder contained in each transponder be denoted by  $\theta$ . Each sub-transponder contains a transmitting side component and a receiving side component [27]. A lightpath occupies a transmitting side component of a sub-transponder at its originating node and a receiving side component of a sub-transponder at its terminating node during its holding time. For the purpose of calculating sub-transponder utilization factor, a transmitting side component and a receiving side component occupied by a lightpath can be counted as one sub-transponder although they are located at different nodes. The sub-transponder utilization factor is calculated as the following ratio

$$\frac{\sum_{p_i \in P} t(p_i)}{\Theta \theta T}. \quad (11)$$

Similarly, the numerator in equation (11) can be accumulated during the simulation whenever a lightpath is torn down.

The average number of existing lightpaths per request is calculated as follows. The number of existing lightpaths used to provision each accepted connection request is counted when each is accepted. The average number of existing lightpaths per request is computed as the ratio of the total number of existing lightpaths used to provision all accepted connection requests to the number of accepted connection requests.

### 5.1. Simulation model

Two network topologies are used in our performance study, namely, the 14-node NSFNET with 21 bidirectional links and the 24-node USNET with 43 bidirectional links as shown in Figs 6(a) and 6(b) respectively. Each link consists of two optical fibers one in each direction. The lengths of the fibers in terms of kilometers are shown on the links in the figures. The total number of available spectrum slots on each fiber is 320 and the width of each

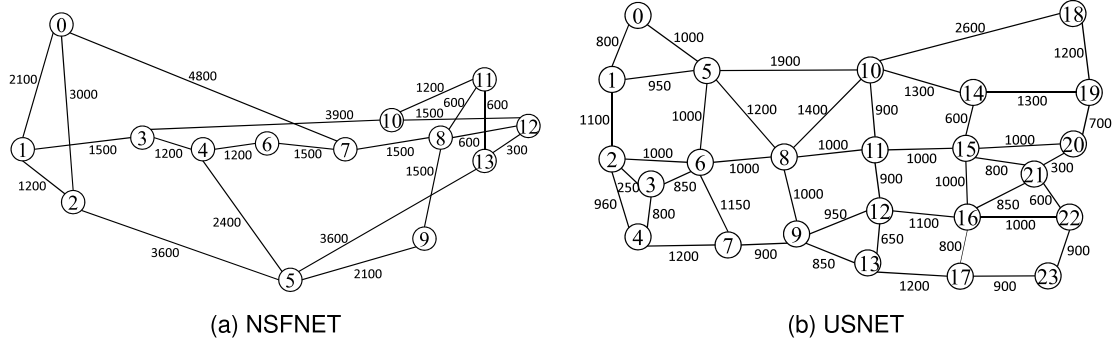


Fig. 6. (a) The topology of the 14-node NSFNET with 21 bidirectional links. (b) The topology of the 24-node USNET with 43 bidirectional links.

spectrum slot is 12.5 GHz. For a lightpath without employing the optical grooming mechanism, guard bands are added on both sides of the traffic slot(s). The width of each guard band is one spectrum slot.

The number of SBVTs in each node is 48 multiplied by the degree of the node. Each SBVT consists of 3 sub-transponders. Each SBVT is able to support up to 10 sub-carriers and 4 modulation formats, namely, BPSK, QPSK, 8-QAM, and 16-QAM. For simplicity, it is assumed that SNR (signal to noise ratio) loss in the EON nodes can be compensated such that transmission reach for a given modulation format is a fixed distance. Techniques for compensation of SNR losses due to various components in the nodes have been discussed in [22]. With the above assumption, the transmission reach for QPSK is selected to be 7,200 Km [7]. The transmission reaches for BPSK, 8-QAM, and 16-QAM are chosen respectively to be 14,400 Km, 3,600 Km and 1,800 Km according to the half-distance law [4].

Connection requests are assumed to arrive at the network according to Poisson process with a mean arrival rate of  $\lambda$  per time unit. Holding times of connection requests are assumed to be exponentially distributed with a mean of one time unit. Bandwidth requirement of each connection request is randomly selected among 10 Gbps, 40 Gbps, 100 Gbps, and 160 Gbps.

The source and destination nodes of each connection request are selected in the following manner. For the NSFNET topology, measured traffic data [21] is used to derive the probabilities for selecting source and destination nodes. The probability that a node is selected as the source node of a connection request is calculated as the ratio of the amount of outgoing traffic of the node to the total amount of outgoing traffic of all nodes. Given a selected source node  $i$ , the probability that node  $j$ ,  $j \neq i$ , is selected as the destination node is computed as the ratio of the amount of traffic from node  $i$  to node  $j$  to the total amount of outgoing traffic of node  $i$ .

For the USNET topology, a guideline for generating non-uniform traffic [26] is used to derive the probabilities for selecting source and destination nodes. The nodes are classified into “Large” nodes and “Small” nodes. Six of the nodes, namely, nodes 5, 6, 8, 10, 15, and 16, are selected as “Large” nodes and the rest of the nodes are “Small” nodes. Traffic distribution among the nodes is as follows: Large-Large: 40%, Large-Small: 40%, Small-Small: 20%. The probabilities for selecting source and destination nodes are calculated based on the traffic distribution.

## 5.2. Comparison of bandwidth blocking ratios

Figures 7(a) and 7(b) compare the bandwidth blocking ratios. It can be observed that all three versions of the proposed MHMP algorithm yield lower bandwidth blocking ratios than the MP-MSU algorithm proposed in [13]. The main reason is that the edge weight on each edge in the auxiliary graph used in the proposed MHMP algorithm is related to the lightpath weights of the set of the lightpaths represented by the edge, which in turn is related to the number of spectrum slots occupied by the lightpaths, spectrum fragmentation, and spectrum misalignment of the set of lightpaths represented by the edge. Whereas spectrum fragmentation and spectrum misalignment are

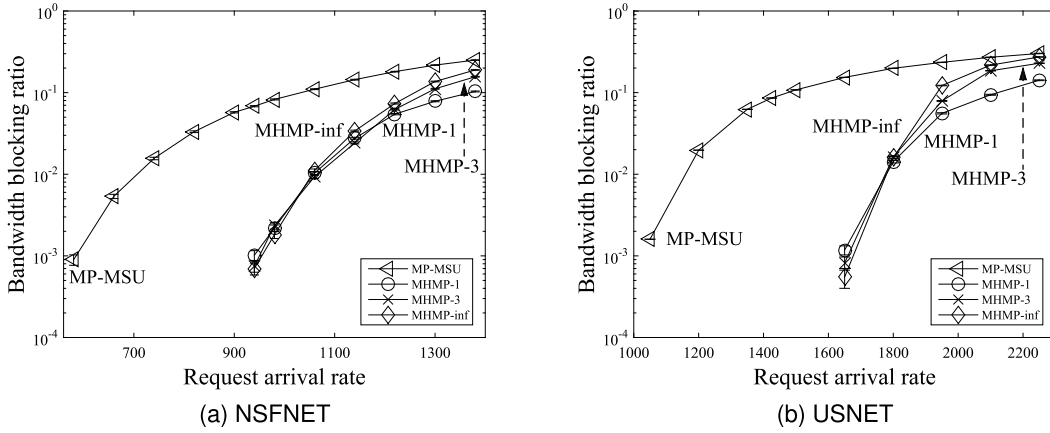


Fig. 7. Comparison of bandwidth blocking ratio.

not considered in the MP-MSU algorithm proposed in [13]. The proposed MHMP algorithm uses the minimum-weight sd-path in the auxiliary graph to provision a connection request implying that lightpaths with less number of spectrum slots, less spectrum fragmentation, and less spectrum misalignment are selected to provision the connection request. Thus, the lightpaths along the minimum-weight sd-path induce less spectrum fragmentation and less spectrum misalignment leading to more useful available spectrum resource for provisioning upcoming connection requests resulting in lower bandwidth blocking ratio.

Comparing the proposed MHMP algorithm with different values for the limit on the number of sd-paths in the auxiliary graphs, when the traffic load is low, in general, the higher the limit on the number sd-paths in the auxiliary graphs the lower the bandwidth blocking ratio. In other words, the MHMP-inf algorithm yields lower bandwidth blocking ratio than the MHMP-3 algorithm and the MHMP-3 algorithm yields lower bandwidth blocking ratio than the MHMP-1 algorithm. The reason is that spectrum resource in the network is abundant when the traffic load is low. With abundant spectrum resource, the proposed MHMP algorithm with higher limit on the number sd-paths is able to use more lightpaths to try to fulfill more connection requests resulting in lower bandwidth blocking ratio. However, when the traffic load is medium to high, spectrum resource in the network is somewhat rare to rare. The proposed MHMP algorithm with lower limit on the number sd-paths uses spectrum resource relatively more conservatively leaving more spectrum resource for upcoming connection requests. Thus, the proposed MHMP algorithm with lower limit on the number sd-paths is able to yield lower bandwidth blocking ratio.

### 5.3. Comparison of spectrum utilization factors

Figures 8(a) and 8(b) show the spectrum utilization factors. It can be observed that, when the traffic load is low, all three versions of the proposed MHMP algorithm yield lower spectrum utilization factors than the MP-MSU algorithm proposed in [13]. The reason is that the proposed MHMP algorithm prefers to utilize residual bandwidths of existing lightpaths to provision connection requests, whereas the MP-MSU algorithm does not give priority to using residual bandwidths of existing lightpaths. When the traffic load is low, it is likely that residual bandwidths of existing lightpaths can be found to provision connection requests without establishing new lightpaths resulting in lower spectrum utilization factors for the three versions of the proposed MHMP algorithm than the MP-MSU algorithm proposed in [13].

As the traffic load increases, residual bandwidths of existing lightpaths and available spectrum slots along sd-paths with smaller number of hops become scarce. Giving priority to using residual bandwidths of existing lightpaths may need to use residual bandwidths of existing lightpaths along sd-paths with larger number of hops requiring more bandwidth for provisioning connection requests. Thus, when the traffic load is high, all three versions of the proposed MHMP algorithm yield higher spectrum utilization factors than the MP-MSU algorithm proposed

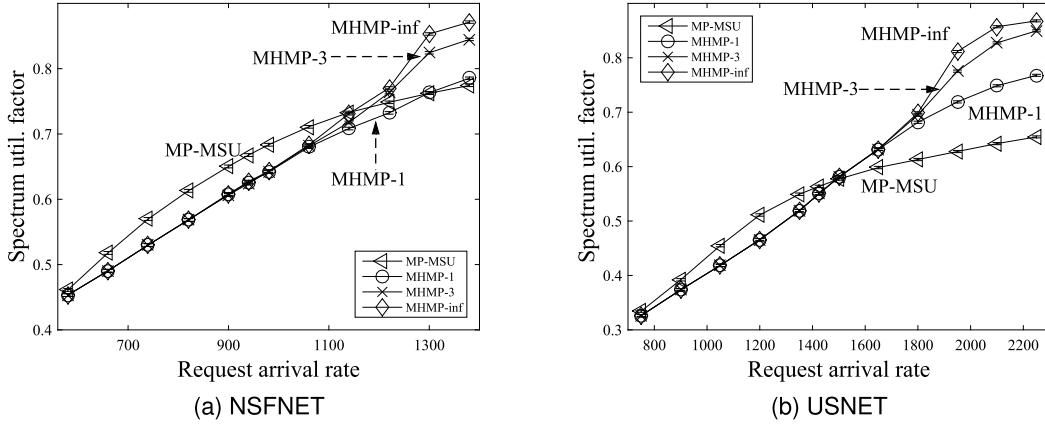


Fig. 8. Comparison of spectrum utilization factors.

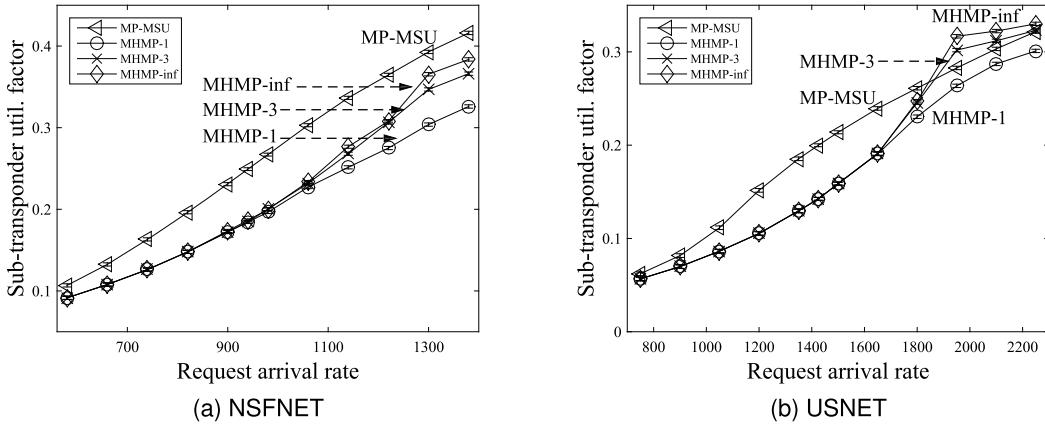


Fig. 9. Comparison of sub-transponder utilization factors.

in [13]. This phenomenon is more evident as the limit on the number  $sd$ -paths increases for the proposed MHMP algorithm. The proposed MHMP algorithm with larger limit on the number  $sd$ -paths yields higher spectrum utilization factor.

#### 5.4. Comparison of sub-transponder utilization factors

Figures 9(a) and 9(b) compare the sub-transponder utilization factors. It can be observed that all three versions of the proposed MHMP algorithm yield lower sub-transponder utilization factors than the MP-MSU algorithm proposed in [13] except when the traffic load is high in the USNET topology. The reason is that all three versions of the proposed MHMP algorithm prefer to use residual bandwidths of existing lightpaths to provision connection requests; i.e., sharing sub-transponders of existing lightpaths is preferable than using free sub-transponders to establish new lightpaths. The MP-MSU algorithm proposed in [13] also employs electrical grooming mechanism; however, no preference is given to using residual bandwidths of existing lightpaths. Hence, all three versions of the proposed MHMP algorithm use electrical grooming mechanism significantly more frequently than the MP-MSU algorithm. Therefore, all three versions of the proposed MHMP algorithm yield lower sub-transponder utilization factors than the MP-MSU algorithm.

When the traffic load is high in the USNET topology, the proposed MHMP algorithm having a limit on the number of sd-path of three or infinity yields higher sub-transponder utilization factor than the MP-MSU algorithm. This is because the USNET topology has larger number of nodes and links compared with the NSFNET topology. Hence, there are more alternatives for finding an sd-path between each pair of nodes in the USNET topology. When the traffic load is high, the residual bandwidths of existing lightpaths and available spectrum slots are scarce along sd-paths with smaller number of hops and smaller number of concatenated lightpaths. The MHMP-3 and MHMP-inf algorithms allow more sd-paths to be used to provision each connection request than the MHMP-1 and MP-MSU algorithms. Therefore, in the USNET topology, it is more likely that the MHMP-3 and MHMP-inf algorithms use sd-paths with larger number of concatenated existing lightpaths or new lightpaths at high traffic load to provision connection requests resulting in occupying larger number of sub-transponders.

### 5.5. Comparison of average number of existing lightpaths per request

Figures 10(a) and 10(b) show the average number of existing lightpaths per request. It can be observed that all three versions of the proposed MHMP algorithm yield higher average number of existing lightpaths per request than the MP-MSU algorithm proposed in [13]. This is because all three versions of the proposed MHMP algorithm prefer to use electrical grooming mechanism to groom traffic of connection requests onto existing lightpaths with residual bandwidths. In contrast, the MP-MSU algorithm proposed in [13] does not give priority to using electrical grooming mechanism although it also employs electrical grooming mechanism.

The two figures also show that the average number of existing lightpaths per request increases as the traffic load increases. As the traffic load increases, on the average, the residual bandwidth of each existing lightpath decreases since the average bandwidth of the traffic carried by each existing lightpath increases when the traffic load increases. With smaller average residual bandwidth in each existing lightpath, it is likely that a larger number of existing lightpaths is used to fulfill a connection request.

Comparing the three versions of the proposed MHMP algorithm, the average number of existing lightpaths per request increases as the limit on the number of sd-paths increases, i.e., the MHMP-inf algorithm yields higher average number of existing lightpaths per request than the MHMP-3 algorithm and the MHMP-3 algorithm yields higher average number of existing lightpaths per request than the MHMP-1 algorithm. The average number of sd-paths used to provision a connection request increases as the limit on the number of sd-paths increases. A larger number of sd-paths is likely to contain a greater number of existing lightpaths. Thus, the average number of existing lightpaths per request increases as the limit on the number of sd-paths increases.

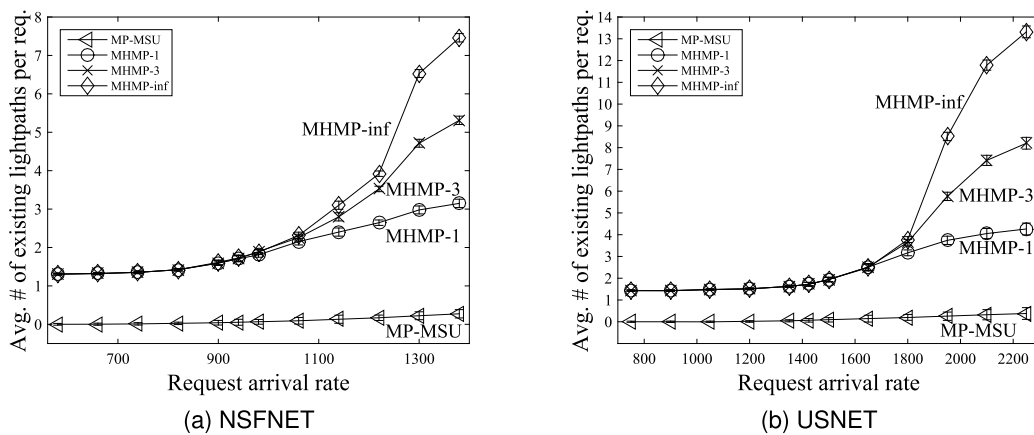


Fig. 10. Comparison of average number of existing lightpaths per request.

## 6. Conclusion

The dynamic multi-hop multipath RMSA and traffic grooming problem in OFDM-based sliceable elastic optical networks has been studied in this paper. A lightpath weight that combines the number of spectrum slots, spectrum fragmentation, and spectrum misalignment has been used to evaluate the potential effect of a lightpath on the availability of network resource. An auxiliary graph has been developed to aid finding source-destination path(s) for provisioning connection requests. Based on the auxiliary graph, this paper has proposed a dynamic multi-hop multipath RMSA and traffic grooming algorithm. Simulation has been carried out to show that the proposed algorithm is able to yield low bandwidth blocking ratio.

## Acknowledgements

This research was supported by the Ministry of Science and Technology, Taiwan, under grant MOST 109-2221-E-007-078.

## Conflict of interest

None to report.

## References

- [1] F.S. Abkenar and A.G. Rahbar, Study and analysis of routing and spectrum allocation (RSA) and routing, modulation and spectrum allocation (RMSA) algorithms in elastic optical networks (EONs), *Opt. Switch. Netw.* **23** (2017), 5–39. doi:10.1016/j.osn.2016.08.003.
- [2] K. Akaki, P. Pavarangoon and N. Kitsuwat, Elastic optical network for fragmented bandwidth allocation with limited slicers, in: *Proceedings of the 13th IEEE International Conference on Information Technology and Electrical Engineering (ICITEE)*, 2021, pp. 1–4.
- [3] R. Alvizu, V. Soto, S. Troia and G. Maier, Enabling multipath optical routing with hybrid differential delay compensation, in: *20th IEEE International Conference on Transparent Optical Networks (ICTON)*, 2018, pp. 1–4.
- [4] A. Bocoi, M. Schuster, F. Rambach, M. Kiese, C.A. Bunge and B. Spinnler, Reach-dependent capacity in optical networks enabled by OFDM, in: *Proc. Optical Networking and Commun. Conf. (OFC)*, 2009.
- [5] A. Cai, L. Peng and G. Shen, Sub-band virtual concatenation lightpath blocking performance evaluation for CO-OFDM optical networks, in: *Proceedings of the OSA Asia Communications and Photonics Conference*, 2012, November, 2012, pp. AS4D-3. doi:10.1364/ACPC.2012.PAF4D.3.
- [6] Y. Cao, A. Almainan, M. Ziyadi, A. Mohajerin-Ariaei, C. Bao, P. Liao, F. Alishahi et al., Reconfigurable channel slicing and stitching for an optical signal to enable fragmented bandwidth allocation using nonlinear wave mixing and an optical frequency comb, *Journal of Lightwave Technology* **36**(2) (2018), 440–446. doi:10.1109/JLT.2017.2750168.
- [7] S. Chandrasekhar, X. Liu, B. Zhu and D.W. Peckham, Transmission of a 1.2-Tb/s 24-carrier no-guard-interval coherent OFDM super-channel over 7200-km of ultra-large-area fiber, in: *Proc. ECOC*, 2009.
- [8] B.C. Chatterjee, N. Sarma and E. Oki, Routing and spectrum allocation in elastic optical networks: A tutorial, *IEEE Commun. Surveys & Tutorials* **17**(3) (2015), 1776–1800. doi:10.1109/COMST.2015.2431731.
- [9] X. Chen, Y. Zhong and A. Jukan, Multipath routing in elastic optical networks with distance-adaptive modulation formats, in: *Proceedings of the IEEE International Conference on Communications (ICC)*, 2013, pp. 3915–3920.
- [10] S. Dahlfort, M. Xia, R. Proietti and S.J.B. Yoo, Split spectrum approach to elastic optical networking, in: *Proceedings of the OSA European Conference and Exhibition on Optical Communication*, 2012, pp. Tu-3.
- [11] Z. Fan, Y. Qiu and C.K. Chan, Dynamic multipath routing with traffic grooming in OFDM-based elastic optical path networks, *Journal of Lightwave Technology* **33**(1) (2015), 275–281. doi:10.1109/JLT.2014.2387312.
- [12] O. Gerstel, M. Jinno, A. Lord and S.B. Yoo, Elastic optical networking: A new dawn for the optical layer?, *IEEE Commun. Mag.* **50**(2) (2012), S12–S20. doi:10.1109/MCOM.2012.6146481.
- [13] S.M.H. Ghazvini, A.G. Rahbar and B. Alizadeh, Load balancing, multipath routing and adaptive modulation with traffic grooming in elastic optical networks, *Computer Networks* **169** (2020), 107081. doi:10.1016/j.comnet.2019.107081.
- [14] T. Hashimoto, K.I. Baba and S. Shimojo, Optical path splitting methods for elastic optical network design, in: *Proceedings of the OSA Asia Communications and Photonics Conference*, 2015, pp. AS4H-4.

- [15] M. Jinno, H. Takara, B. Kozicki, Y. Tsukishima, Y. Sone and S. Matsuoka, Spectrum-efficient and scalable elastic optical path network: Architecture, benefits, and enabling technologies, *IEEE Commun. Mag.* **47**(11) (2009), 66–73. doi:[10.1109/MCOM.2009.5307468](https://doi.org/10.1109/MCOM.2009.5307468).
- [16] M. Jinno, H. Takara, Y. Sone, K. Yonenaga and A. Hirano, Multi-flow optical transponder for efficient multilayer optical networking, *IEEE Commun. Mag.* **50**(5) (2012), 56–65. doi:[10.1109/MCOM.2012.6194383](https://doi.org/10.1109/MCOM.2012.6194383).
- [17] N. Kadu, S. Shakya and X. Cao, Modulation-aware multipath routing and spectrum allocation in elastic optical networks, in: *Proceedings of the IEEE International Conference on Advanced Networks and Telecommunications Systems (ANTS)*, 2014, pp. 1–6.
- [18] N. Kitsuwon, K. Akaki, P. Pavarangkoon and A. Nag, Spectrum allocation scheme considering spectrum slicing in elastic optical networks, *Journal of Optical Communications and Networking* **13**(7) (2021), 169–181. doi:[10.1364/JOCN.422915](https://doi.org/10.1364/JOCN.422915).
- [19] N. Malpani and J. Chen, A note on practical construction of maximum bandwidth paths, *Information Processing Letters* **83**(3) (2002), 175–180. doi:[10.1016/S0020-0190\(01\)00323-4](https://doi.org/10.1016/S0020-0190(01)00323-4).
- [20] S. Miladić-Tešić, G. Marković and V. Radojčić, Traffic grooming technique for elastic optical networks: A survey, *Optik* **176** (2019), 464–475. doi:[10.1016/j.ijleo.2018.09.068](https://doi.org/10.1016/j.ijleo.2018.09.068).
- [21] B. Mukherjee, D. Banerjee and S. Ramamurthy, Some principles for designing a wide-area WDM optical network, *IEEE/ACM Trans. Netw.* **4**(5) (1996), 684–696. doi:[10.1109/90.541317](https://doi.org/10.1109/90.541317).
- [22] A. Napoli, D. Rafique, M. Bohn, N. Nölle, J.K. Fischer and C. Schubert, Transmission in elastic optical networks, in: *Elastic Optical Networks*, Springer, Cham, 2016, pp. 83–116.
- [23] A. Pagès, J. Perelló, S. Spadaro and J. Comellas, Optimal route, spectrum, and modulation level assignment in split-spectrum-enabled dynamic elastic optical networks, *Journal of Optical Communications and Networking* **6**(2) (2014), 114–126. doi:[10.1364/JOCN.6.000114](https://doi.org/10.1364/JOCN.6.000114).
- [24] A. Pagès, J. Perelló, S. Spadaro and G. Junyent, Split spectrum-enabled route and spectrum assignment in elastic optical networks, *Optical Switching and Networking* **13** (2014), 148–157. doi:[10.1016/j.osn.2014.04.002](https://doi.org/10.1016/j.osn.2014.04.002).
- [25] L. Ruiz, R.J.D. Barroso, I. De Miguel, N. Merayo, J.C. Aguado and E.J. Abril, Routing, modulation and spectrum assignment algorithm using multi-path routing and best-fit, *IEEE Access* **9** (2021), 111633–111650. doi:[10.1109/ACCESS.2021.3101998](https://doi.org/10.1109/ACCESS.2021.3101998).
- [26] A.A.M. Saleh, Dynamic multi-terabit core optical networks: Architecture, protocols, control and management (CORONET), in: *DARPA BAA*, 2006, pp. 06-29.
- [27] N. Sambo, P. Castoldi, A. D’Errico, E. Riccardi, A. Pagano, M.S. Moreolo, J.M. Fabrega et al., Next generation sliceable bandwidth variable transponders, *IEEE Communications Magazine* **53**(2) (2015), 163–171. doi:[10.1109/MCOM.2015.7045405](https://doi.org/10.1109/MCOM.2015.7045405).
- [28] S. Talebi, F. Alam, I. Katib, M. Khamis, R. Salama and G.N. Rouskas, Spectrum management techniques for elastic optical networks: A survey, *Optical Switching and Networking* **13** (2014), 34–48. doi:[10.1016/j.osn.2014.02.003](https://doi.org/10.1016/j.osn.2014.02.003).
- [29] U. Ujjwal, N. Mahala and J. Thangaraj, Dynamic adaptive spectrum allocation in flexible grid optical network with multi-path routing, *IET Communications* **15** (2021), 211–223. doi:[10.1049/cmu2.12046](https://doi.org/10.1049/cmu2.12046).
- [30] X. Wang, G. Shen, Z. Zhu and X. Fu, Benefits of sub-band virtual concatenation for enhancing availability of elastic optical networks, *Journal of Lightwave Technology* **34**(4) (2016), 1098–1110. doi:[10.1109/JLT.2015.2509605](https://doi.org/10.1109/JLT.2015.2509605).
- [31] Y. Yin, H. Zhang, M. Zhang, M. Xia, Z. Zhu, S. Dahlfort and S.B. Yoo, Spectral and spatial 2D fragmentation-aware routing and spectrum assignment algorithms in elastic optical networks, *IEEE/OSA Journal of Optical Communications and Networking* **5**(10) (2013), A100–A106. doi:[10.1364/JOCN.5.00A100](https://doi.org/10.1364/JOCN.5.00A100).
- [32] Y. Yin, M. Zhang, Z. Zhu and S.J.B. Yoo, Fragmentation-aware routing, modulation and spectrum assignment algorithms in elastic optical networks, in: *Proceedings of the OSA Optical Fiber Communication Conference*, 2013, pp. OW3A-5.
- [33] F. Yousefi and A.G. Rahbar, Novel fragmentation-aware algorithms for multipath routing and spectrum assignment in elastic optical networks-space division multiplexing (EON-SDM), *Optical Fiber Technology* **46** (2018), 287–296. doi:[10.1016/j.yofte.2018.11.002](https://doi.org/10.1016/j.yofte.2018.11.002).
- [34] F. Yousefi, A.G. Rahbar and M. Yaghubi-Namaad, Fragmentation-aware algorithms for multipath routing and spectrum assignment in elastic optical networks, *Optical Fiber Technology* **53** (2019), 102019. doi:[10.1016/j.yofte.2019.102019](https://doi.org/10.1016/j.yofte.2019.102019).
- [35] G. Zhang, M. De Leenheer and B. Mukherjee, Optical traffic grooming in OFDM-based elastic optical networks [invited], *Journal of Optical Commun. and Networking* **4**(11) (2012), B17–B25. doi:[10.1364/JOCN.4.000B17](https://doi.org/10.1364/JOCN.4.000B17).
- [36] Y. Zhang, L. Li, Y. Li, S.K. Bose and G. Shen, Spectrally efficient operation of mixed fixed/flexible-grid optical networks with sub-band virtual concatenation, in: *Proceedings of the IEEE 18th International Conference on Transparent Optical Networks (ICTON)*, 2016, pp. 1–4.
- [37] R. Zhu, J.P. Jue, A. Yousefpour, Y. Zhao, H. Yang, J. Zhang, X. Yu and N. Wang, Multi-path fragmentation-aware advance reservation provisioning in elastic optical networks, in: *Proceedings of the IEEE Global Communications Conference (GLOBECOM)*, 2016, pp. 1–6.
- [38] R. Zhu, Y. Zhao, H. Yang, X. Yu, J. Zhang, A. Yousefpour, N. Wang and J.P. Jue, Dynamic time and spectrum fragmentation-aware service provisioning in elastic optical networks with multi-path routing, *Optical Fiber Technology* **32** (2016), 13–22. doi:[10.1016/j.yofte.2016.08.009](https://doi.org/10.1016/j.yofte.2016.08.009).
- [39] Z. Zhu, W. Lu, L. Zhang and N. Ansari, Dynamic service provisioning in elastic optical networks with hybrid single-/multi-path routing, *Journal of Lightwave Technology* **31**(1) (2013), 15–22. doi:[10.1109/JLT.2012.2227683](https://doi.org/10.1109/JLT.2012.2227683).